

# Quantitative analysis of sphingolipids for lipidomics using triple quadrupole and quadrupole linear ion trap mass spectrometers<sup>§</sup>

Rebecca L. Shaner,\* Jeremy C. Allegood,<sup>1,\*</sup> Hyejung Park,<sup>†</sup> Elaine Wang,<sup>†</sup> Samuel Kelly,<sup>†</sup> Christopher A. Haynes,<sup>†</sup> M. Cameron Sullards,<sup>\*,†</sup> and Alfred H. Merrill, Jr.<sup>2,\*†</sup>

Schools of Chemistry and Biochemistry,\* and Biology,<sup>†</sup> Petit Institute for Bioengineering and Bioscience, Georgia Institute of Technology, Atlanta, GA 30332-0230

**Abstract** Sphingolipids are a highly diverse category of bioactive compounds. This article describes methods that have been validated for the extraction, liquid chromatographic (LC) separation, identification and quantitation of sphingolipids by electrospray ionization, tandem mass spectrometry (ESI-MS/MS) using triple quadrupole (QQQ, API 3000) and quadrupole-linear-ion trap (API 4000 QTrap, operating in QQQ mode) mass spectrometers. Advantages of the QTrap included: greater sensitivity, similar ionization efficiencies for sphingolipids with ceramide versus dihydroceramide backbones, and the ability to identify the ceramide backbone of sphingomyelins using a pseudo-MS<sup>3</sup> protocol. Compounds that can be readily quantified using an internal standard cocktail developed by the LIPID MAPS Consortium are: sphingoid bases and sphingoid base 1-phosphates, more complex species such as ceramides, ceramide 1-phosphates, sphingomyelins, mono- and di-hexosylceramides, and these complex sphingolipids with dihydroceramide backbones. With minor modifications, glucosylceramides and galactosylceramides can be distinguished, and more complex species such as sulfatides can also be quantified, when the internal standards are available. **LC ESI-MS/MS** can be utilized to quantify a large number of structural and signaling sphingolipids using commercially available internal standards. The application of these methods is illustrated with RAW264.7 cells, a mouse macrophage cell line. These methods should be useful for a wide range of focused (sphingo)lipidomic investigations.—Shaner, R. L., J. C. Allegood, H. Park, E. Wang, S. Kelly, C. A. Haynes, M. C. Sullards, and Alfred H. Merrill, Jr. **Quantitative analysis of sphingolipids for lipidomics using triple quadrupole and quadrupole linear ion trap mass spectrometers.** *J. Lipid Res.* 2009. 50: 1692–1707.

**Supplementary key words** lipid maps • lipidomics internal standards • mass spectrometry • RAW 264.7 macrophage • sphingolipids

This work was supported by the Lipid MAPS Consortium "Glue" Grant U54-GM069338.

\*Author's Choice—Final version full access.

Manuscript received 18 November 2008.

Published, JLR Papers in Press, November 25, 2008  
DOI 10.1194/jlr.D800051-JLR200

Sphingolipids are an amazingly complex family of compounds found in eukaryotes as well as some prokaryotes and viruses. They are involved in many aspects of cell structure, metabolism, and regulation (1, 2). Many methods have been used for sphingolipid analysis, from classic methods such as TLC (3) and HPLC (4) to mass spectrometry (MS), which has proven to be useful for analysis of broad categories of sphingolipids from sphingoid bases and their 1-phosphates (5–8) to ceramides (Cer) (6, 9–12), sphingomyelins (SM) (13–18), simple mono- and dihexosylceramides (15, 19–22), and more complex glycosphingolipids (23–29). Some of the MS methods are applicable for lipidomic ("sphingolipidomic") studies because they are able to profile subspecies in multiple categories (6, 7, 15, 30–34), especially when tandem mass spectrometry (MS/MS) with electrospray ionization (ESI) is combined with liquid chromatography (LC) to minimize overlap of isomers such as glucosylceramide (GlcCer) and galactosylceramide (GalCer) (15, 34).

Quantitative analysis of lipids by mass spectrometry requires internal standards to control for variability in recovery from the biological material and factors that can affect ion yield. The ideal internal standard is a stable isotope-

Abbreviations: CE, collision energies; Cer, ceramide; Cer1P, ceramide 1-phosphate; CXP, collision cell exit potentials; DHCer, dihydroceramide; DHCer1P, dihydroceramide 1-phosphate; DHSM, dihydrosphingomyelin; DP, declustering potential; EP, entrance potential; FBS, fetal bovine serum; FP, focusing potential; GalCer, galactosylceramide; GlcCer, glucosylceramide; HexCer, hexosylceramide; LC, liquid chromatographic; LacCer, lactosylceramide; LC-MS/MS, liquid chromatography tandem mass spectrometry; MRM, multiple reaction monitoring; PBS, phosphate-buffered saline; Q, quadrupole; QQQ, triple quadrupole; QTrap, quadrupole linear-ion trap; SM, sphingomyelin; Sa, sphinganine; Sa1P, sphinganine 1-phosphate; So, sphingosine; SIP, sphingosine 1-phosphate.

<sup>1</sup>Present address of J. C. Allegood: Department of Biochemistry and Molecular Biology, Virginia Commonwealth University School of Medicine, Richmond, VA 23298-5048

<sup>2</sup>To whom correspondence should be addressed.

email: al.merrill@biology.gatech.edu

<sup>§</sup>The online version of this article (available at <http://www.jlr.org>) contains supplementary data in the form of 13 figures.

labeled version of each analyte of interest, but it is impractical for these to be used for the large numbers of compounds examined in a lipidomic study. Therefore, an alternative is to identify internal standards that are similar in structure and ionization and fragmentation characteristics for the categories of compounds under investigation. This study evaluates an internal standard cocktail (now commercially available) developed for the LIPID MAPS Consortium (34) that contains uncommon chain-length sphingoid bases (C17) for sphingosine (So), sphinganine (Sa) and the 1-phosphates (S1P and Sa1P) and C12:0 fatty acid analogs of Cer (and, as discussed in the text, the cocktail initially also had C25:0-Cer), ceramide 1-phosphate (Cer1P), SM and mono- and dihexosylCer (HexCer and diHexCer). Examples are also given for how the types of analytes can be expanded by supplementation with additional internal standards. Because it is common in mass spectrometry for laboratories to have different categories of instruments available, this article describes the optimization and validation of the sphingolipid internal standard cocktail by electrospray tandem mass spectrometry on two types of instruments, a triple quadrupole mass spectrometer and a quadrupole linear-ion trap mass spectrometer, both operating in the triple quadrupole modes. The analytes of interest were identified and quantified by LC ESI-MS/MS using multiple reaction monitoring (MRM), a technique where the eluate is repetitively scanned for selected precursor-product ion pairs to enhance the sensitivity and specificity of the analysis. The method is applicable to relatively small samples (e.g., a Petri dish of cells), as exemplified by analysis of RAW264.7 cells, a mouse macrophage cell line.

## MATERIALS AND METHODS

### Materials

The LIPID MAPS™ internal standard cocktail (initially Sphingolipid Mix I, catalog number LM-6002; later replaced by Sphingolipid Mix II, catalog number LM-6005 as explained under “Results”) was provided by Avanti Polar Lipids (Alabaster, AL) in sealed ampules and certified (35) to be over 95% pure and within 10% of the specified amount (25 μM). It was composed of the 17-carbon chain length sphingoid base analogs C17-sphingosine, (2S,3R,4E)-2-aminoheptadec-4-ene-1,3-diol (d17:1-So)<sup>3</sup>; C17-sphinganine, (2S,3R)-2-aminoheptadecane-1,3-diol (d17:0-Sa); C17-sphingosine 1-phosphate, heptadecaphing-4-ene-1-phosphate (d17:1-So1P); and C17-sphinganine 1-phosphate, heptadecaphing-4-ene-1-phosphate (d17:0-Sa1P); and the C12-fatty acid analogs of the more complex sphingolipids C12-Cer, N-(dodecanoyl)-sphing-4-ene (d18:1/C12:0); C12-Cer 1-phosphate, N-(dodecanoyl)-sphing-4-ene-1-phosphate (d18:1/C12:0-Cer1P); C12-sphingomyelin, N-(dodecanoyl)-sphing-4-ene-1-phosphocholine (d18:1/C12:0-SM); C12-glucosylceramide, N-(dodecanoyl)-1-β-glucosyl-sphing-4-ene (d18:1/C12:0-GlcCer); and C12-lactosylceramide, N-(dodecanoyl) 1-β-lactosyl-sphing-4-ene (d18:1/

C12:0-LacCer); as well as one very-long-chain Cer analog, C25-Cer, N-(pentacosanoyl)-sphing-4-ene (d18:1/C25:0), which was added initially but later removed for reasons described under “Results.”

The other chain-length subspecies of these sphingolipids, which were compared with the internal standards, as well as internal standards for sulfatides (d18:1/C12:0-sulfatide, ST) and GalCer (d18:1/C12:0-GalCer), were obtained from Avanti and Matreya (Pleasant Gap, PA). When the dihydro- (i.e., sphinganine backbone) versions of the standards were not commercially available, they were synthesized by reduction of the backbone double bond using hydrogen gas and 10% Pd on charcoal (Aldrich-Sigma, St. Louis, MO) (36) and verification that the conversion was complete by LC ESI-MS/MS.

The HPLC grade solvents (acetonitrile, # EM-AX0145; chloroform, # EM-CX1050; hexane, # JT9304-33; and methanol, # EM-MX0475, as well as formic acid (ACS grade, # EM-FX0440-7), were obtained from VWR (West Chester, PA), and acetic acid (ACS grade, # A38C-212) was obtained from Fischer (Pittsburg, PA).

### Cell culture

RAW264.7 cells, a macrophage-like cell line derived from tumors induced in male BALB/c mice by the Abelson murine leukemia virus (37), were obtained from the American Type Culture Collection (Manassas, VA) (cat# TIB-71; lot# 3002360), stored as frozen stocks to ensure the cells were never passaged more than 20 times, and cultured according to LIPID MAPS protocols ([www.lipidmaps.org](http://www.lipidmaps.org)), as briefly summarized here. The cells were grown in 60 mm plastic culture dishes in DMEM supplemented with 10% FBS, 4 mM L-glutamine, 4.5 g/L glucose, 1.5 g/L sodium bicarbonate, 100 U/ml penicillin, and 0.1 mg/ml streptomycin. RAW264.7 cells were cultured at 37°C, 95% relative humidity, and 5% CO<sub>2</sub> in a ThermoForma SteriCult CO<sub>2</sub> incubator. Cells that were at 80% confluence were rinsed with phosphate buffered saline (PBS), scraped from the dish, and seeded at 2.5 × 10<sup>6</sup> cells in 5 ml of media in 60 mm dishes, and analyzed after 24 h. The cells were quantified by DNA assay using the Quant-iT DNA Assay Kit, Broad Range (Molecular Probes, cat #Q-33130).

### Lipid extraction from RAW264.7 cells

The cells were washed twice with PBS, with the dishes tilted to aid in the removal of as much liquid as possible. Then the cells were scraped from the dish in the residual PBS (typically < 0.2 ml)<sup>4</sup> using Nalgene cell scrapers (Rochester, NY) and transferred into 13 × 100 mm borosilicate tubes with a Teflon-lined cap (catalog #60827-453, VWR, West Chester, PA). After adding 0.5 ml of CH<sub>3</sub>OH and 0.25 ml of CHCl<sub>3</sub>, the internal standard cocktail (500 pmol of each species dissolved in a final total volume of 10 μl of ethanol) were added, and the contents were dispersed using a Branson 1510 ultra sonicator (Sigma) at room temperature for 30 s. This single phase mixture was incubated at 48°C overnight in a heating block, which affords optimal extraction of sphingolipids due to their high phase transition temperatures (3). After cooling, 75 μl of 1 M KOH in CH<sub>3</sub>OH was added and, after brief sonication, incubated in a shaking water bath for 2 h at 37°C to cleave potentially interfering glycerolipids. After cooling to room temperature, approximately 3 to 6 μl of glacial acetic

<sup>3</sup>This nomenclature designates the backbone sphingoid base by number of hydroxyls (e.g., d = di-) and carbon atoms:double bonds; if there is an amide-linked fatty acid, it is designated by “C” followed by the number of carbon atoms:double bonds.

<sup>4</sup>If the cells are recovered in a larger volume, the volumes of the other steps must be increased proportionately; or in some cases, the cells can be removed from dishes and centrifuged to reduce the volume, if this does not disrupt membrane integrity, as assessed by a method such as (trypan blue) dye exclusion.

acid was added to bring the extract to neutral pH (checked with pH paper to ensure that the extract has been neutralized),<sup>5</sup> and a 0.4-ml aliquot was transferred to a new test tube to serve as the "single-phase extract" (which was centrifuged to remove the insoluble residue, the supernatant collected, the residue reextracted with 1 ml of methanol:CHCl<sub>3</sub>, 1:2, *v:v*, centrifuged, and the supernatants combined). To the remainder of the original extract was added 1 ml of CHCl<sub>3</sub> and 2 ml of H<sub>2</sub>O followed by gentle mixing then centrifugation using a table-top centrifuge, and the lower layer (the "organic-phase extract") was transferred to a new tube. The upper phase was extracted with an additional 1 ml of CHCl<sub>3</sub>, which was also added to the organic-phase extract.

The solvents were removed from the single-phase extract and the organic-phase extract using a Savant AES2000 Automatic Environmental Speed Vac. The dried residue was reconstituted in 0.3 ml of the appropriate mobile phase solvent for LC-MS/MS analysis (described herein and the summary in Fig. 1), sonicated for approximately 15 s, then transferred to a microcentrifuge tube and centrifuged at 14,000 to 16,000 *g* for several min (as needed) before transfer of the clear supernatant to the autoinjector vial for analysis.

### Liquid chromatographic separation conditions for different subcategories of sphingolipids

Summarized in Fig. 1 are the types of LC columns and extraction conditions that were found to be optimal for analysis of different subcategories of sphingolipids that are often encountered in mammalian cells, such as the RAW264.7 cell line. This scheme illustrates, nonetheless, that the investigator has multiple options depending on the nature of the biological sample; for example, if a particular biological sample contains only GlcCer (as is the case for RAW264.7 cells under standard culture conditions), then a shorter amino-column can be used, but if GlcCer and GalCer are both present, an additional run with a longer silica column will also be necessary to distinguish these isomers. Specific LC conditions and instrument parameters for specific analytes are described herein. For all methods, 0.03–0.05 ml were injected onto the column.

*Sphingoid bases, sphingoid base 1-phosphates, and ceramide 1-phosphates.* These compounds were analyzed using the single-phase extract because their recovery into the organic phase of a traditional lipid extraction can be variable. They were separated by reverse phase LC using a Supelco 2.1 (i.d.) × 50 mm Discovery C18 column (Sigma, St. Louis, MO) and a binary solvent system at a flow rate of 1.0 ml/min. If this flow rate does not afford complete desolvation (typically seen as a jagged elution profile), the flow rate can be reduced and/or the ion source gas flow rate can be increased.

Prior to injection of the sample, the column was equilibrated for 0.4 min with a solvent mixture of 60% Mobile phase A1 (CH<sub>3</sub>OH/H<sub>2</sub>O/HCOOH, 58/41/1, *v/v/v*, with 5 mM ammonium formate) and 40% Mobile phase B1 (CH<sub>3</sub>OH/HCOOH, 99/1, *v/v*, with 5 mM ammonium formate), and after sample injection (typically 50 μL), the A1/B1 ratio was maintained at 60/40 for 0.5 min, followed by a linear gradient to 100% B1 over 1.8 min, which was held at 100% B1 for 5.3 min, followed by a 0.5 min wash of the column with 60:40 A1/B1 before the next run.

<sup>5</sup>This differs from previous reports from our laboratory where neutralization of the single phase extract was not necessary, however, we are now finding some degradation unless this is done. Whether this is due to contaminants in the test tubes, a shift in the temperature of the Speed Vac, etc., has not been ascertained.

The elution times for these analytes (Fig. 2) are discussed under "Results."

In cases where there is significant carryover of Cer1P on this LC column (i.e., over 1%, which occurs with reverse phase columns obtained from some suppliers as well as with some lots of the columns described in this article), Cer1P can be analyzed instead using a Supelco 2.1 (i.d.) × 50 mm Discovery C8 column (Sigma, St. Louis, MO), with the column heated to 60°C and a binary solvent system [based on reference (38)] at a flow rate of 0.6 ml/min. Prior to the injection, the column is equilibrated for 2 min with a solvent mixture of 70% Mobile phase altA1 (CH<sub>3</sub>OH/H<sub>2</sub>O/THF/HCOOH, 68.5/28.5/2/1, *v/v/v*, with 5 mM ammonium formate) and 30% Mobile phase altB1 (CH<sub>3</sub>OH/THF/HCOOH, 97/2/1, *v/v/v*, with 5 mM ammonium formate), and after sample injection (30 μL), the altA1/altB1 ratio is maintained at 70/30 for 0.4 min, followed by a linear gradient to 100% altB1 over 1.9 min, which is held at 100% altB1 for 5.3 min, followed by a 0.5 min wash of the column with 70:30 altA1/altB1 before the next run.

*Ceramides, sphingomyelins, monohexosylceramides (HexCer) and dihexosylceramides (LacCer).* These compounds were analyzed using the organic-phase extract and normal-phase LC using a Supelco 2.1 (i.d.) × 50 mm LC-NH<sub>2</sub> column at a flow rate of 1.0 ml/min and a binary solvent system as shown in Fig. 2C. Prior to injection, the column was equilibrated for 1.0 min with 100% Mobile phase A2 (CH<sub>3</sub>CN/CH<sub>3</sub>OH/HCOOH, 97/2/1, *v/v/v*, with 5 mM ammonium formate), and after sample injection, Mobile phase A2 was continued for 3 min, followed by a 1.0-min linear gradient to 100% Mobile phase B2 (CH<sub>3</sub>OH/H<sub>2</sub>O/HCOOH, 89/6/5, *v/v/v*, with 50 mM triethylammonium acetate), which was held for 3.0 min, then restored to 100% A2 by a 1.0-min linear gradient, and maintained at 100% A2 for 1 min to reequilibrate the column. In addition to these analytes, Cer1P and sulfatides (ST) can also be analyzed, however, their recoveries are higher in the single-phase extract, which can be reconstituted in the solvent for normal phase chromatography (Mobile phase A2). The elution times for these analytes are discussed under "Results."

*Resolution of glucosylceramide (GlcCer) and galactosylceramide (GalCer).* If the biological sample contains both GlcCer and GalCer (the latter is less widely distributed, and only found in barely detectable amounts in RAW264.7 cells until stimulation with Kdo<sub>2</sub>-Lipid A, as described under "Results"), these can be resolved using a different normal phase column (Supelco 2.1 (i.d.) × 250 mm LC-Si) and an isocratic elution with Mobile phase A3 (CH<sub>3</sub>CN/CH<sub>3</sub>OH/H<sub>3</sub>CCOOH, 97/2/1, *v/v/v*, with 5 mM ammonium acetate) at 1.5 ml per min (this can be reduced to 0.75 ml/min if necessary for complete desolvation). After the column is preequilibrated for 1.0 min, the sample (dissolved in Mobile phase A3) is injected, and the column is isocratically eluted for 8 min. In most cases, the GlcCer and GalCer are separated by 0.5–1 min (as shown in Fig. 2D), which should be confirmed during the analysis by interspersing vials with these internal standards throughout the runs.

*Other sphingolipids (sulfatides).* Sulfatides were analyzed using the same normal phase chromatography as described for SM, GlcCer, etc. (Fig. 2C); however, prior to extraction, the samples were spiked with 500 pmol of C12-sulfatide (d18:1/C12-GalSulfate) (from Avanti Polar Lipids). The organic-phase extract can be used for a qualitative screen of whether or not sulfatides are present, but for quantitation, a separate run should be made using the single-phase extract because it has the higher recovery (over 50%).

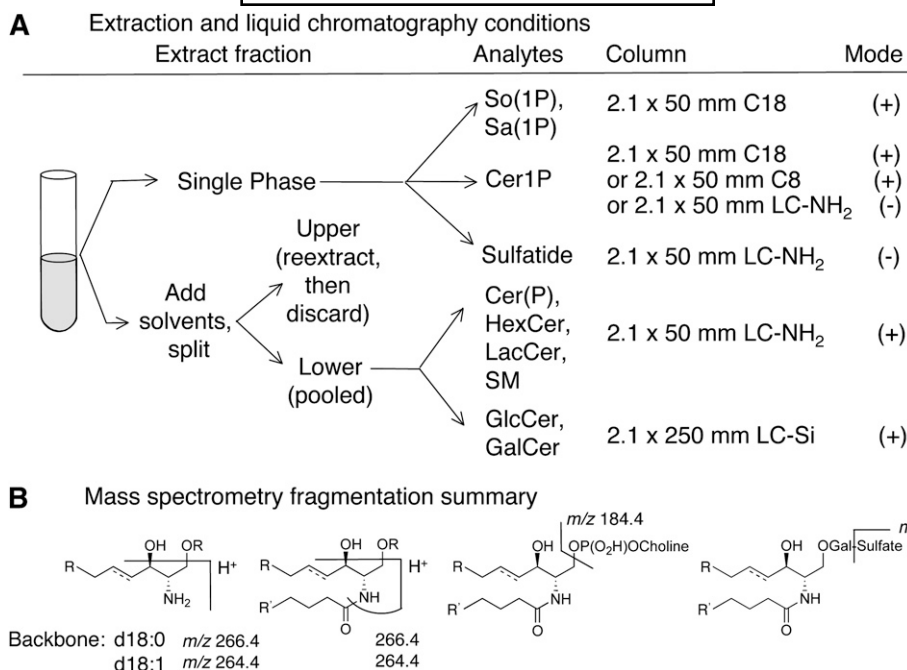


**Fig. 1.** Workflow diagram for sample preparation for analysis of different categories of sphingolipids by LC-MS/MS. A: After addition of organic solvents to form a single phase and base hydrolysis (at far left), half of the sample is used as the “single-phase extract” for analysis of the shown categories of sphingolipids and the other half is further extracted to obtain a lower (organic) phase for the other categories. For more details, see “Materials and Methods.” B: Depiction of the major fragmentations of different categories of sphingolipids described in this article. For the sphingoid bases and ceramides depicted in the left two structures, -OR = -OH, -phosphate or mono- or di-hexosyl groups at position 1, and R and R’ are the alkyl sidechains for the sphingoid base and fatty acid, respectively, which can vary in length and, to some extent, unsaturation.

### Mass spectrometric analysis of standards and biological samples

Two systems were used for these analyses: a Perkin Elmer Series 200 MicroPump system coupled to a PE Sciex API 3000 triple quadrupole (QQQ) mass spectrometer (Applied Biosystems, Foster City, CA), and a Shimadzu LC-10 AD VP binary pump system coupled to a Perkin Elmer Series 200 autoinjector coupled to a 4000 quadrupole linear-ion trap (QTrap) (Applied Biosystems, Foster City, CA) operating in a triple quadrupole mode. For both instruments, Q1 and Q3 were set to pass molecularly distinctive precursor and product ions (or a scan across multiple  $m/z$  in Q1 or Q3), using N<sub>2</sub> to collisionally induce dissociations in Q2 (which was offset from Q1 by 30–120 eV); the ion source temperature varied between 300 and 500°C depending on solvent composition and mass spectrometer.

*Identification of ionization and fragmentation parameters for standards and analytes.* As the LC conditions were established (described above), the optimal conditions for ionization and fragmentation were determined for each analyte, and standard curves were established. Each sphingolipid standard was dissolved at a concentration of 1–10 pmol/μL in the appropriate solvent mixture in which it elutes from the column and infused into the ion source at a rate of 0.6 ml/h to determine the optimal ionization conditions by varying the declustering potential (DP) and focusing potential (FP) for the API3000, and the DP and entrance potential (EP) for the 4000 QTrap. After the Q1 settings were determined, product ion spectra were collected across a range of collision energies (CE), structurally specific product ions were identified, and collision energies and collision cell exit potentials (CXP) were manipulated to produce optimal signal

for the product ion of choice. Mass spectrometer conditions can also be optimized by injecting the sample via a sample loop with the solvents present at elution time at the given flow rate to better mimic LC conditions. Once the settings were identified (see Tables 1–4), the precursor/product ion pairs (based on the characteristic fragmentations shown in Fig. 1B) were placed in MRM methods as described herein.

*Survey of subspecies in biological samples for selection of the Multiple Reaction Monitoring (MRM) parameters.* As the analysis of sphingolipids in cell extracts was conducted in MRM mode where specific precursor-product pairs are monitored during the LC elution, it is necessary first to scan a representative cell extract to determine which subspecies are present. This should be conducted over a wide enough range that sphingoid base and acyl-chain subspecies that are shorter (e.g., C16-sphingoid base and C14:0 fatty acyl) as well as longer (such as the C20-sphingoid base and C30-fatty acyl-chain length ceramides, the latter being found in skin) would be detected. If tissues contain significant amounts of subspecies that are outside the range described in this report, the investigator will need to determine the optimal parameters for the additional species using the appropriate standards.

To perform the subspecies survey, the extract was resuspended in 0.5 ml of CH<sub>3</sub>OH and infused into the 4000 QTrap (which was the more sensitive instrument) at 0.6 ml/h and a scan of precursors for  $m/z$  184.4 was used to detect the subspecies of SM, and scans of the precursors for  $m/z$  264.4 (d18:1 backbone) and 266.4 (d18:0 backbone) were performed over a wide range of collision energies (35–75 eV) to check for other subspecies of sphingolipids. This also detects subspecies with a 4-hydroxysphinganine (phytosphingosine, t18:0) backbone and/or an α-hydroxy-fatty acid because these have a 16 amu higher precursor  $m/z$  and also

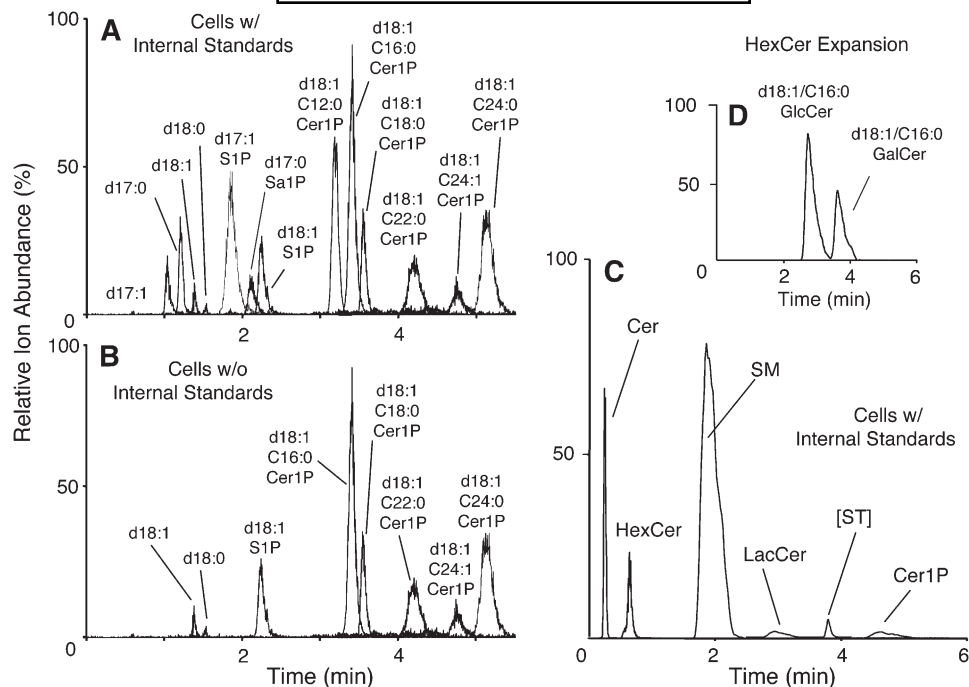


**Fig. 2.** LC ESI-MS/MS elution profiles for the sphingolipids on reverse phase (A, B) and normal phase (C, D) chromatography. Shown are the elution of sphingoid bases and 1-phosphates and Cer1P in the single-phase extract of approximately  $1 \times 10^6$  RAW 264.7 cells with internal standard cocktail (500 pmol of each internal standard) (panel A) versus cells alone (panel B) from a Supelco 2.1mm i.d.  $\times$  5 cm Discovery C18 column and analysis by MRM in positive ionization mode as described under “Materials and Methods.” The abbreviations identify the nature of the sphingoid base (e.g., S, sphingosine, d18:1; Sa, sphinganine, d18:0; and internal standards d17:1 and d17:0), the 1-phosphates (1P), and ceramide 1-phosphates (Cer1P, designating the sphingoid base and amide-linked fatty acid). C: Elution of complex sphingolipids in the “lower phase extract” of approximately  $1 \times 10^6$  RAW264.7 cells from a Supelco 2.1 mm i.d.  $\times$  5 cm LC-NH<sub>2</sub> column and analysis by MRM in positive ion mode for Cer to LacCer, then negative ion mode for ST and Cer1P. D: Separation of d18:1/C16:0-GlcCer and -GalCer standards using a Supelco 2.1mm i.d.  $\times$  25 cm LC-Si column and the conditions described under “Materials and Methods.”

produce a  $m/z$  264.4 fragment (that can later be distinguished from the d18:1 species by LC mobility); to check for other sphingoid base backbones, the product  $m/z$  is varied by  $\pm 14$  amu for likely homologs (e.g.,  $-14$  for 17:1 and  $+28$  for 20:1) and by  $-2$  amu for additional unsaturation (e.g., d18:2). The results from these surveys are used to construct the MRM protocol for analysis of the cell extracts by LC-MS/MS (see Tables 1–4) in which Q1 and Q3 were set to pass the precursor and most abundant, structurally specific product ion for each sphingolipid subspecies (for example,  $m/z$  538.7/264.4, 566.5/264.4, 594.6/264.4, 622.7/264.4, 648.7/264.4, 650.7/264.4 for d18:1/C16:0, d18:1/C18:0, d18:1/C20:0, d18:1/C22:0, d18:1/C24:1, and d18:1/C24:0 ceramides, respectively). The dwell time was 25 ms for each transition, which provided at least 4 data points per s of elu-

tion time when MRM pairs were being monitored for 8 analytes in a given period. Both Q1 and Q3 were set to unit resolution.

*Standard curves for quantitative analysis of sphingolipids by LC-MS/MS.* Once the LC and MRM protocols were selected, standard curves were determined under these conditions. The concentration of the individual components of the Avanti internal standard cocktail was 25  $\mu$ M and the other sphingolipid subspecies were dissolved in methanol to produce stocks at 0.5 mg/ml. These were serially diluted into the appropriate LC solvent immediately before analysis to provide 0.5–1000 pmol of each standard per 50  $\mu$ L injection. Each was then analyzed by LC-MS/MS in each of the mass spectrometers to generate the standard curves such as those shown in the figures and supplementary figures of

TABLE 1. API 3000 mass spectrometer settings for long chain bases and phosphates and linear regressions

	Q1 $m/z$	Q3 $m/z$	DP (V)	FP (V)	CE (V)	R <sup>2</sup>
d17:1 So	286.4	250.3	30	180	28	0.996
d17:0 Sa	288.4	252.4	30	180	28	0.993
d18:1 So	300.4	264.4	30	180	35	0.997
d18:0 Sa	302.4	266.4	30	180	35	0.997
d17:1 S1P	366.4	250.3	30	180	30	0.999
d17:0 Sa1P	368.4	252.4	30	180	30	0.992
d18:1 S1P	380.4	264.4	30	180	35	0.994
d18:0 Sa1P	382.4	266.4	30	180	35	0.991

CE, collision energies; DP, declustering potential; FP, focusing potential; Q, quadrupole; So, sphingosine; Sa, sphinganine; S1P, sphingosine 1-phosphate; Sa1P, sphinganine 1-phosphate.

TABLE 2. 4000 QTrap mass spectrometer settings for long chain bases and phosphates and linear regressions

	Q1 <i>m/z</i>	Q3 <i>m/z</i>	DP (V)	CE (V)	CXP (V)	R <sup>2</sup>
d17:1 So	286.4	268.3	40	15	15	0.999
d17:0 Sa	288.4	60.0	50	45	9	0.995
d18:1 So	300.4	282.4	40	21	16	0.996
d18:0 Sa	302.4	60.0	50	50	10	0.994
d17:1 SIP	366.4	250.3	50	23	16	0.994
d17:0 Sa1P	368.4	252.2	50	25	16	0.997
d18:1 SIP	380.4	264.4	50	25	16	0.993
d18:0 Sa1P	382.4	266.4	50	25	16	0.998

CE, collision energies; CXP, collision cell exit potentials; DP, declustering potential; Q, quadrupole; So, sphingosine; Sa, sphinganine; SIP, sphingosine 1-phosphate; Sa1P, sphinganine 1-phosphate.

this article, then to calculate the linear regression lines and fit in Tables 1–4.

*Quantitative analysis of sphingolipids in cell extracts by LC-MS/MS.* To quantify the amounts of the sphingolipid analytes of interest in cell extracts, the elution profiles for each MRM pair were examined. The areas under the peaks generated for both analytes and internal standards can then be integrated with the mass spectrometer software (i.e., Analyst 1.4.2 for both Applied Biosystems instruments). Using identical integration settings (number of

smooths = 2–3, bunching factor = 5–10, and noise threshold =  $1 \times 10^4$ ) to integrate both internal standard and analyte allowed quantitation to obtain the areas under the curves, then the pmol of the analyte was calculated using the following formula:

pmol of analyte of interest =  $K_{\text{analyte}} \times (A_{\text{analyte}} / A_{\text{IS}}) \times \text{pmol of added internal standard}$

where  $K_{\text{analyte}}$  = correction factor for the analyte versus the internal standard;  $A_{\text{analyte}}$  = area of the analyte; and  $A_{\text{IS}}$  = area of the added internal standard. The  $K_{\text{analyte}}$  factor adjusts for differences between the analyte and the internal standard with respect to ion yield per

TABLE 3. API 3000 mass spectrometer settings for complex sphingolipids and linear regressions

	N-Acyl	Q1 <i>m/z</i>	Q3 <i>m/z</i>	DP (V)	FP (V)	CE (V)	R <sup>2</sup>
Cer	C12:0	482.6	264.4	40	220	35	0.996
	C16:0	538.7	264.4	40	220	40	0.997
	C18:0	566.7	264.4	40	220	42.5	0.999
	C24:1	648.9	264.4	40	220	45	0.998
	C24:0	650.9	264.4	40	220	45	0.997
DHCer	C25:0	664.9	264.4	40	220	47.5	0.999
	C16:0	540.7	266.4	40	220	40	0.996
	C18:0	568.7	266.4	40	220	42.5	0.992
	C24:1	650.9	266.4	40	220	45	0.997
GlcCer	C24:0	652.9	266.4	40	220	45	0.996
	C12:0	644.6	264.4	50	300	45	0.991
	C16:0	700.7	264.4	50	300	50	0.994
	C18:0	728.7	264.4	50	300	52.5	0.996
DHGlcCer	C24:1	810.9	264.4	50	300	60	0.990
	C12:0	646.6	266.4	50	300	45	0.992
	C16:0	702.7	266.4	50	300	50	0.993
	C18:0	730.7	266.4	50	300	52.5	0.997
SM	C24:0	814.9	266.4	50	300	60	0.994
	C12:0	647.7	184.4	20	200	40	0.999
	C18:0	731.8	184.4	20	200	45	0.999
	C24:0	815.9	184.4	20	200	50	0.998
DHSM	C12:0	649.7	184.4	20	200	40	0.998
	C18:0	733.8	184.4	20	200	45	0.997
	C24:0	817.9	184.4	20	200	50	0.998
Cer1P (pos)	C12:0	562.6	264.4	40	220	45	0.992
	C16:0	618.7	264.4	40	220	50	0.990
	C24:0	730.9	264.4	40	220	55	0.997
DHCer1P (pos)	C12:0	564.6	266.4	40	220	50	0.994
	C24:0	732.9	266.4	40	220	55	0.996
Cer1P (neg)	C12:0	560.6	78.9	–35	–180	70	0.993
	C16:0	616.7	78.9	–35	–180	75	0.991
	C24:0	728.9	78.9	–35	–180	80	0.995
DHCer1P (neg)	C16:0	562.6	78.9	–35	–180	75	0.999
	C24:0	730.9	78.9	–35	–180	80	0.992
	C12:0	722.4	96.9	–55	–140	110	0.999
Sulfatide	C16:0	778.6	96.6	–55	–140	115	0.993
	C24:0	890.9	96.9	–55	–140	120	0.995
	C12:0	806.6	264.4	40	220	50	0.991
LacCer	C16:0	862.7	264.4	40	220	55	0.995
	C24:0	974.9	264.4	40	220	60	0.989

CE, collision energies; Cer, ceramide; Cer1P, ceramide 1-phosphate; DHCer, dihydroceramide; DHCer1P, dihydroceramide 1-phosphate; DHSM, dihydrosphingomyelin; DP, declustering potential; FP, focusing potential; GlcCer, glucosylceramide; LacCer, lactosylceramide; Q, quadrupole; SM, sphingomyelin.

TABLE 4. 4000 QTrap mass spectrometer settings for complex sphingolipids and linear regressions

	N-Acyl	Q1 <i>m/z</i>	Q3 <i>m/z</i>	DP (V)	CE (V)	CXP (V)	R <sup>2</sup>
Cer	C12:0	482.6	264.4	55	35	15	0.994
	C16:0	538.7	264.4	55	37.5	15	0.997
	C18:0	566.7	264.4	55	37.5	15	0.992
	C24:1	648.9	264.4	55	42.5	15	0.996
	C24:0	650.9	264.4	55	42.5	15	0.997
	C25:0	664.9	264.4	55	45	15	0.997
DHCer	C16:0	540.7	266.4	55	37.5	15	0.990
	C18:0	568.7	266.4	55	37.5	15	0.995
	C24:1	650.9	266.4	55	42.5	15	0.989
	C24:0	652.9	266.4	55	42.5	15	0.992
GlcCer	C12:0	644.6	264.4	35	42.5	15	0.996
	C16:0	700.7	264.4	35	45	15	0.995
	C18:0	728.7	264.4	35	47.5	15	0.995
	C24:1	810.9	264.4	35	55	15	0.987
DHGlcCer	C12:0	646.6	266.4	35	42.5	15	0.995
	C16:0	702.7	266.4	35	45	15	0.990
	C18:0	730.7	266.4	35	47.5	15	0.998
	C24:0	814.9	266.4	35	55	15	0.986
SM	C12:0	647.7	184.4	45	40	10	0.997
	C18:0	731.8	184.4	45	45	10	0.996
	C24:0	815.9	184.4	45	50	10	0.999
DHSM	C12:0	649.7	184.4	45	40	10	0.999
	C18:0	733.8	184.4	45	45	10	0.994
	C24:0	817.9	184.4	45	50	10	0.999
Cer1P (pos)	C12:0	562.6	264.4	40	45	15	0.996
	C16:0	618.7	264.4	40	47.5	15	0.993
	C24:0	730.9	264.4	40	52.5	15	0.995
DHCer1P (pos)	C12:0	564.6	266.4	40	47.5	15	0.992
	C24:0	732.9	266.4	40	52.5	15	0.985
Cer1P (neg)	C12:0	560.6	78.9	-120	-60	-15	0.996
	C16:0	616.7	78.9	-120	-65	-15	0.993
	C24:0	728.9	78.9	-120	-72.5	-15	0.997
DHCer1P (neg)	C16:0	562.6	78.9	-120	-65	-15	0.998
	C24:0	730.9	78.9	-120	-72.5	-15	0.995
Sulfatide	C12:0	722.4	96.9	-220	-100	-15	0.994
	C16:0	778.6	96.9	-220	-110	-15	0.999
	C24:0	890.9	96.9	-220	-125	-15	0.995
LacCer	C12:0	806.6	264.4	45	55	15	0.990
	C16:0	862.7	264.4	45	60	15	0.987
	C24:0	974.9	264.4	45	70	15	0.986

CE, collision energies; Cer, ceramide; Cer1P, ceramide 1-phosphate; CXP, collision cell exit potentials; DHCer, dihydroceramide; DHCer1P, dihydroceramide 1-phosphate; DHSM, dihydrosphingomyelin; DP, declustering potential; GlcCer, glucosylceramide; LacCer, lactosylceramide; Q, quadrupole; SM, sphingomyelin.

unit amount for the selected MRM pair, which also includes any correction for differences in isotopic abundance (~1.1% per carbon), which are insignificant for analytes with alkyl chain lengths similar to the internal standard but become more substantial for very-long-chain species. If the chain length is outside the number that have been corrected thus (i.e., for which there is an internal standard that can be used to determine the correction factor empirically), one can adjust the difference in isotopic distribution from the nearest standard using the ratio of (M+H)<sup>+</sup>, (M+H+1)<sup>+</sup>, and (M+H+2)<sup>+</sup> for the number of carbons in the analyte versus the internal standard using Analyst 1.4.2 or an online tool such as <http://www2.sisweb.com/mstools/isotope.htm>.

No correction was necessary for differences in extraction recovery because the extraction conditions were chosen to achieve similar recoveries, as described herein. Following the LIPID MAPS convention, the quantities of the sphingolipids are expressed as pmol/μg of DNA. For comparison, it has been our experience that 1 × 10<sup>6</sup> RAW 264.7 cells contain approximately 3 μg of DNA and approximately 0.25 mg of protein.

#### Optimization of sphingolipid recovery from cells in culture

To determine the number of extraction steps necessary for recovery of the sphingolipids from RAW264.7 cells, the solid resi-

due from the single-phase extract and the aqueous layer from the organic-phase extract were reextracted three times using the above method, and each extract was analyzed by LC-MS/MS. To validate the extraction protocol, ~3.0 × 10<sup>6</sup> RAW 264.7 cells (N = 6) were spiked with internal standards and extracted, with repeated reextraction of the residue at the sphingoid base step and with repeated aqueous reextracts of the organic layer at the complex sphingolipid step. Using the optimized protocol, the reproducibility of the method was determined by analyzing three separate series of cultured RAW264.7 cells (six dishes prepared separately on three different days) and the coefficient of variation (CV) was calculated as the SD divided by the mean × 100.

#### Quality control

For each LC analysis, vials with the internal standards alone were analyzed at the beginning, middle, and end of the run. In addition, blank samples (containing only the LC solvent) were analyzed at varying intervals throughout the run to assess possible carryover. If carryover or shifts in the LC retention times for any of the analytes or standards were noticed, the column was cleaned before resuming the run. As noted above, some columns had an unacceptable level of carryover of Cer1P, and when that was the case, that analyte was reanalyzed using the alternative method.

## RESULTS

The goal of these experiments was to test the utility of a commercially available internal standard cocktail for the quantitation of cellular sphingolipids using LC-MS/MS and two types of instruments, an API 3000 triple quadrupole (QQQ) mass spectrometer and a 4000 quadrupole linear-ion trap (QTrap) mass spectrometer in triple quadrupole mode. To achieve this objective, many of the LC-MS/MS conditions from previous publications (15, 34) were used; however, a number of minor modifications were identified during these studies, such as the observation that carryover of Cer1P occurs on some reverse phase columns.

The sections below describe the order in which each category of internal standard and analyte was evaluated, starting with identification of the fragmentation profiles for selection of the precursor-product pairs, optimization of the parameters for LC-MS/MS, and application of the methods to cells, with the additional tests for extraction efficiencies.

### Identification of major ions and fragments for LIPID MAPS™ internal standards and related analytes

Syringe infusion was used to select precursor/product ion pairs for MRM based on the structure-specific ions that were of highest intensity under optimized conditions. As noted previously (15, 34), most of the sphingolipids (Cer, Cer1P, HexCer and sphingoid bases) and their dihydro-counterparts fragment to backbone ions with  $m/z$  264.4 (for d18:1) or  $m/z$  266.4 (for d18:0) in positive ion mode as shown in Fig. 1B (and in supplementary Figs. I–III for Cer, HexCer, and Hex<sub>2</sub>Cer), whereas the most abundant product ion from CID of (dihydro)SM was  $m/z$  184.4 from the choline phosphate headgroup (Fig. 1B and supplementary Fig. IV), and from sulfatides, the loss of sulfate [ $(\text{HSO}_4^-)$ ,  $m/z$  96.9 (supplementary Fig. VI)]. The fragmentation profiles for the internal standards and the corresponding analytes were also similar under optimized conditions described herein.

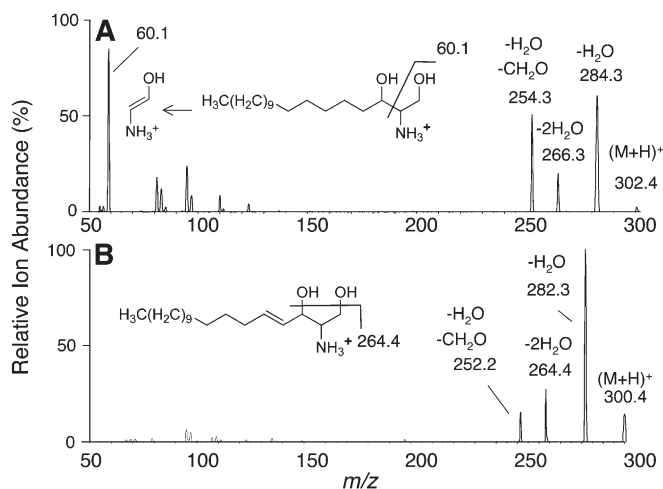


**Fig. 3.** Product ion scans of sphinganine (A) and sphingosine (B) using the 4000 QTrap. Samples were infused in methanol.

There were some interesting differences between the instruments. Most notably, in the 4000 QTrap, the single dehydration product [ $(m/z$  284.3 (Fig. 3A)] and a small fragment with  $m/z$  60.1 ( $\text{C}_2\text{H}_6\text{NO}$  from cleavage of the C2-C3 bond) were abundant ions for sphinganine [and the single dehydration product was also abundant for sphingosine,  $m/z$  282.3 (Fig. 3B)]; whereas in the API 3000, sphingosine and sphinganine yielded primarily  $m/z$  264.4 and 266.4 fragments (7, 15, 34). The C2-C3 bond cleavage product is useful for identification of 1-deoxysphingoid bases (i.e., to establish that they are 1-deoxy- and not 3-deoxy-compounds), which have been found in various biological systems (39), because they are cleaved to  $m/z$  44.1 (data not shown).

There were also differences in sensitivity that are discussed later, however, the greater sensitivity of the 4000 QTrap in negative ionization mode allowed analysis of Cer1P in both positive (supplementary Fig. V-A) and negative (supplementary Fig. V-B) ionization mode. Sulfatides were also analyzed in negative ion mode, with loss of sulfate ( $m/z$  96.8) as the major product ion (supplementary Fig. V).

These fragmentation characteristics were used to select the MRM pairs used to optimize the LC and mass spectrometer settings in Tables 1–4.

### Optimization of LC ESI-MS/MS conditions

Using an initial set of ionization parameters for the MRM pairs for the selected sphingolipids, the LC conditions shown in Fig. 2 were devised, then the ionization parameters were optimized to ensure that they were appropriate for the electrospray solvent composition of the LC eluate. Standard curves for each analyte category were then determined by LC-MS/MS with the results described herein.

*Sphingoid bases and sphingoid base 1-phosphates.* Using the LC conditions for analysis of these compounds (Fig. 2), the ionization and CID conditions for the internal standards and analytes were optimized. The results are summarized in Tables 1 and 2. The highest recoveries of these compounds were obtained in the single-phase extract fraction (described herein); therefore, it was consistently used for analysis of these compounds (although the lower phase organic solvent extract could also be used, with this caveat regarding the lower recovery).

Graphs of the integrated ion intensities from these MRM analyses versus amounts for the sphingoid bases and sphingoid base 1-phosphates (both the naturally occurring d18 and the internal standard d17) species are shown for the API 3000 and 4000 QTrap (Fig. 4). Using both instruments, all of the species showed a linear signal response of 0.5–1000 pmol, and the d17 and d18 species behaved similarly. The major difference in signal response was for saturated and unsaturated species (e.g., d18:1 versus d18:0), which confirms the need for internal standards for each. The 4000 QTrap was approximately 3–4 orders of magnitude more sensitive for analysis of these compounds than the API 3000.



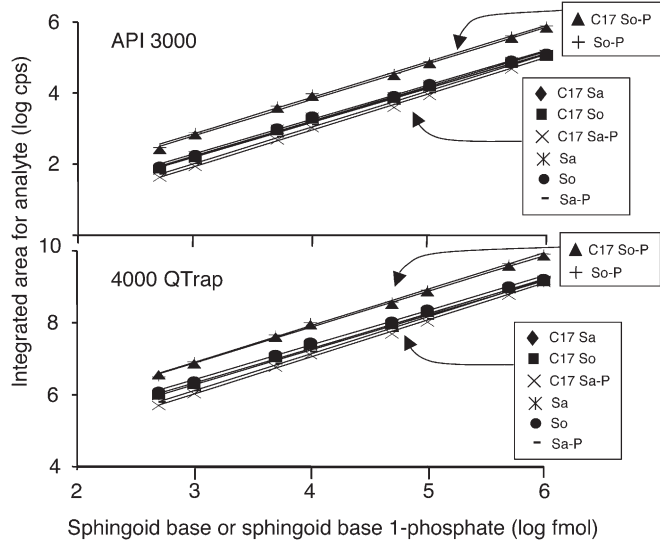


**Fig. 4.** Signal response for sphingoid bases and sphingoid base 1-phosphates using the ABI 3000 (QQQ) and 4000 QTrap. Each compound was analyzed over the shown range in amounts on column using the LC-MS/MS protocol for sphingoid bases and phosphates on reverse phase chromatography and positive ion mode MS/MS using optimized ionization, fragmentation, and MRM conditions as described under “Materials and Methods.”

**Ceramides.** These compounds were analyzed using the lower phase organic solvent extract (information about extraction recoveries are described herein). Graphs of the integrated ion intensities for these analytes and standards versus amounts (0.5–1000 pmol) are shown in **Fig. 5** for Cer (d18:1) with N-acyl chain lengths from C12:0 to C25:0 (panels A and B) and for dihydroCer (d18:0) with C16 to C24 (panels C and D). Using these LC conditions (Fig. 2) and optimized ionization parameters (Tables 3 and 4), all of the subspecies displayed a linear signal response of 0.5–1000 pmol on both instruments, with little difference in cps due to the length of the fatty acyl-chain.

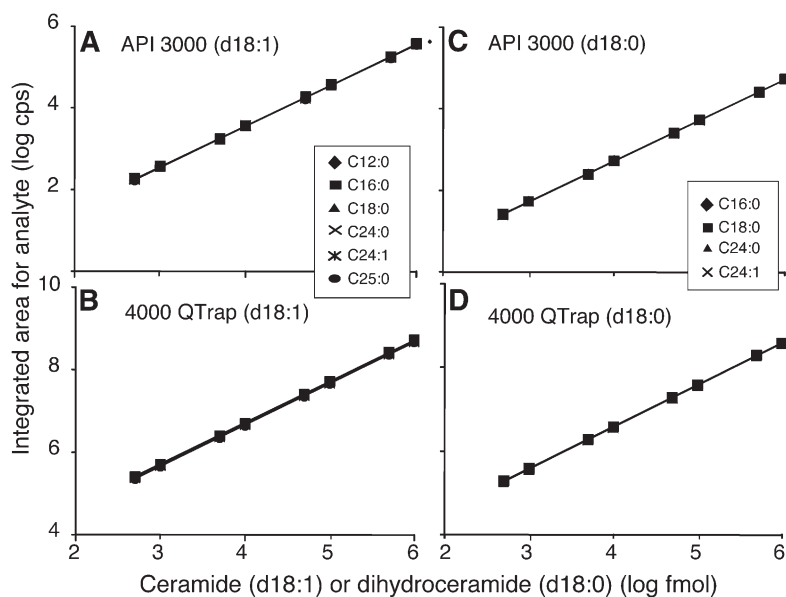


**Fig. 5.** Signal response for varying N-acyl chain length Cer (d18:1) and dihydroCer (d18:0) using the API 3000 (QQQ) and 4000 QTrap. Each compound was analyzed over the shown range in amounts on column using normal phase LC and positive ion mode MS/MS using optimized ionization, fragmentation, and MRM conditions as described under “Materials and Methods.”

The 4000 QTrap was several orders of magnitude more sensitive than the API 3000 for these compounds. In addition, in the 4000 QTrap, the ion yields for DHCer were close (~85%) to the corresponding Cer (c.f. Fig. 5, panels B and D) whereas the ion yields for Cer on the QQQ were 6–8 times higher than their respective dihydroCer (c.f. Fig. 5, panels A and C), although this is somewhat difficult to discern due to the log scale. In the API 3000, there was also a slightly greater difference between the C12-Cer and C25-Cer (4%).

The similarity in signal response across all these chain lengths (C12:0–C25:0) and for both Cer and dihydroCer using the 4000 QTrap allows the C12:0 internal standard to be used for all of these species (with a small correction for the 15% difference noted above). The same is the case for the API 3000, but with a larger correction factor (6- to 8-fold for DHCer versus Cer, and 4% for C12- to C25Cer). The initial LIPID MAPS™ sphingolipid internal standard cocktail included C25-Cer to provide an empirical confirmation of this chain-length difference within each run. However, during studies of the RAW264.7 cells, we noted a discrepancy in the amounts of C24:1-Cer (d18:1/C24:1) using the API 3000 versus the 4000 QTrap that was caused by in-source dehydration of C25-Cer. This was surprising because the precursor-product pair of the in-source dehydration product of C25-Cer ( $m/z$  646.9/264.4) does not correspond to the MRM pair for C24:1-Cer (Tables 1–4), however, the M+2  $^{13}\text{C}$  isotopologue of C25-Cer ( $m/z$  648.9/264.4) provides this match. This explanation was confirmed by analysis of the internal standard alone and by reverse phase LC-MS/MS (data not shown). Even though this interference can be minimized by careful selection of the ionization and fragmentation parameters for the instrument (indeed, these must be optimized for maximal sensitivity for the cellular ceramides), if other investigators find that this artifact is produced in their mass spectrometer, they should use an internal standard cocktail mix without C25-Cer. This mix is now available from

Avanti Polar Lipids as LIPID MAPS™ sphingolipid internal standard Mix II (Catalog number, LM-6005).

**Sphingomyelins.** These compounds were analyzed using the lower phase organic solvent extract (information about extraction recoveries are described herein). After identification of LC conditions for analysis of these compounds (Fig. 2) and optimization of the ionization parameters (Tables 3 and 4), SM (d18:1) and dihydroSM (d18:0) with N-acyl chain lengths of C12:0–C24:0 were analyzed (supplementary Fig. VII). All of the subspecies displayed a linear signal response of 0.5–1000 pmol on both instruments, and there was little difference in cps due to the length of the fatty acyl-chain. The signal response for SM on the 4000 QTrap (supplementary Fig. VII-B) was approximately an order of magnitude higher than for the API 3000 (supplementary Fig. VII-A). Because SM and dihydroSM are analyzed by loss of the phosphocholine headgroup rather than backbone cleavage, the cps for the saturated and unsaturated backbone was similar for both instruments.

Although the positive ion mode CID does not allow definitive determination of fatty acid and sphingoid base combinations of SM (i.e., they are only inferred once the biological material is found to have little or no sphingoid base chain length variants), we have noticed that one can utilize the trap functionalities of the 4000 QTrap in negative ion mode to produce cleavage products with backbone information (Fig. 6). This is done by selecting the same precursor ion  $m/z$  for the first and second product ion, then offsetting  $Q_2$  by 5–10 eV so that no fragmentation occurs in the collision cell. Precursors are then induced to fragment in the ion trap by application of an amplitude frequency, allowing observation of structurally indicative peaks. This pseudo-MS<sup>3</sup> enhances the backbone structure specific fragment ( $m/z$  449.4 in Fig. 6B) versus the amount of this fragment in typical MS/MS mode (c.f. Fig. 6B versus Fig. 6A), and thus allows postrun analysis of the SM in a sample for structural verification.

Since SM is much more abundant than any of the other sphingolipids, it was more prone to showing a loss of linearity in the ion intensity versus amount (data not shown). We did not ascertain if this is due to column overloading or ionization suppression; however, it was readily detected and rectified by analyzing the lipid extracts in several different dilutions (e.g., full strength and as a 1/10 dilution of the LC mobile phase used for sample injection).

**Monohexosylceramides.** These compounds were analyzed using the lower phase organic solvent extract (information about extraction recoveries are described herein). After identification of LC conditions<sup>6</sup> for analysis of these compounds (Fig. 2) and optimization of the ionization parameters (Tables 3 and 4), both GlcCer (d18:1) and dihy-

<sup>6</sup>If high back pressure is encountered when using the GlcCer/GalCer method (i.e., chromatography on a 2.1 x 250 mm LC-Si column as described in Fig. 1A and the text) with the 4000 QTrap with the Turbo V ion source, this can be circumvented by adjusting the flow rate to 0.75  $\mu\text{L}/\text{min}$ .

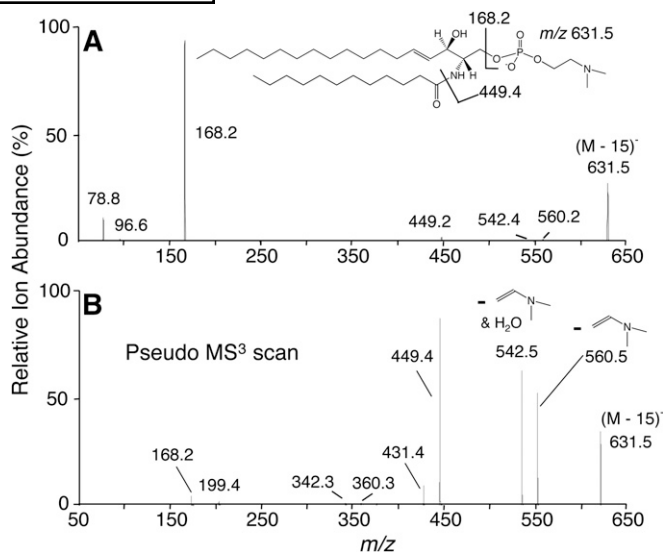


**Fig. 6.** Comparison of sphingomyelin product ion by traditional negative ion mode MS/MS in the 4000 QTrap (A) and by “pseudo MS<sup>3</sup>” analysis (B). Panel A is the product ion scan for the major precursor ion,  $m/z$  631.5 from the in-source demethylation of SM; panel B reflects the results that are obtained by selecting the same precursor ion  $m/z$  for the first and second product ion, then offsetting  $Q_2$  by 5–10 eV so that no fragmentation occurs in the collision cell. Precursors are then induced to fragment in the ion trap by application of an amplitude frequency, allowing observation of the peaks shown when scanned as a “pseudo MS<sup>3</sup>.”

droGlcCer (d18:0) with N-acyl chain lengths C12:0–C24:1 were analyzed (supplementary Fig. VIII). All of the subspecies displayed a linear signal response of 0.5–1000 pmol on both instruments. There was little difference in cps due to the length of the fatty acyl-chain. Overall signal for GlcCer was approximately 2.5 orders of magnitude higher on the 4000 QTrap versus the API 3000, and little correction is needed for the dihydro backbone in the 4000 QTrap, whereas for the API 3000, an 8-fold correction factor is needed (supplementary Fig. VIII).

Comparisons of standard GlcCer and GalCer with comparable backbones did not reveal any differences in ion yield (data not shown); therefore, the C12-GlcCer internal standard is adequate for analysis of total HexCer (i.e., where the stereochemistry of the carbohydrate is not specified). This might not be the case, however, for other backbones, such as ones with  $\alpha$ -hydroxy-fatty acids. Many cells do not contain galacto-family sphingolipids, so it is not necessary to distinguish GlcCer and GalCer in many instances, although the ability to do so using the modified LC conditions described under “Materials and Methods” (see Fig. 2D) allows this analysis when needed. Since GalCer may be present in trace amounts compared with GlcCer, the separation of these compounds by LC should have greater sensitivity than a shotgun approach that distinguishes them in mixtures by only differences in the peak intensity ratio of the product ions at  $m/z$  179 and 89 (31).

**Dihexosylceramides (lactosylceramides).** These compounds were analyzed using the lower phase organic solvent extract (information about extraction recoveries are de-

scribed herein). After identification of LC conditions for analysis of these compounds (Fig. 2) and optimization of the ionization parameters (Tables 3 and 4), both LacCer (d18:1) and dihydroLacCer (d18:0) with C16:0 and C24:0 acyl chains, as well as the C12-LacCer internal standard, were analyzed (supplementary Fig. IX). All of the species displayed a linear signal response of 0.5–1000 pmol on both instruments. There was little difference in cps due to the length of the fatty acyl-chain. Therefore, the C12- internal standard can be used within this range of alkyl-chain lengths. Signal response for LacCer is the lowest of the sphingolipids observed in positive ion mode (supplementary Fig. IX), with approximately an order of magnitude greater sensitivity in the 4000 QTrap than API 3000. When analyzed using the 4000 QTrap, the cps for dihydroLacCer (d18:0) was only 20% lower than for LacCer (d18:1), but it was approximately 5-fold lower for the d18:0 versus d18:1 backbone species using the API 3000.

**Ceramide 1-phosphates.** The highest recoveries of these compounds were obtained in the single-phase extract (described herein), therefore, they were used for quantitative analysis.<sup>7</sup> The elution profiles for Cer-P on reverse phase and normal phase LC are shown in Fig. 2. Reverse phase chromatography was selected because it was compatible with the high salt in the single-phase extract and positive ionization mode ESI-MS/MS gives the more structure-specific fragmentation (i.e., cleavage to the sphingoid base backbone ions versus loss of phosphate in negative ionization mode). Once the LC conditions were selected, ionization and CID conditions for the internal standards and analytes were optimized. The results are summarized in Tables 3 and 4. Graphs of the integrated ion intensities from these MRM analyses versus amounts are shown in supplementary Fig. X for both Cer1P (d18:1) and dihydroCer1P (d18:0) with C16:0 and C24:0 acyl chains, compared with the C12-Cer1P internal standard. All species displayed a linear signal response of 0.5–1000 pmol on both instruments. There was little difference in cps due to the length of the fatty acyl-chain. Therefore, the C12-internal standard can be used with Cer1P within this range of alkyl-chain lengths. The 4000 QTrap is approximately an order of magnitude more sensitive than the API 3000 for analysis of Cer1P (supplementary Fig. X).

Because we have sometimes encountered significant (i.e., as high as 10%) carryover of Cer1P using some lots of the reverse-phase C18 chromatographic material, an LC method using another solid phase (C8) has been developed for those instances (see “Materials and Methods”). The LC conditions for complex sphingolipids (Fig. 2C) can also be used to analyze Cer1P, but the elution peaks are broad.

*Analysis of additional sphingolipids by modification of these protocols, as exemplified by sulfatides.* As an example of how it should be possible to analyze additional sphingolipids by

<sup>7</sup>The lower phase organic solvent extract can also be used for screening or confirmation since the low recovery (ca 10 to 20%) can be corrected using the internal standard, however, the most reliable results are obtained using the single-phase extract, where the recovery is over 90% as shown in Fig. 10).

supplementation of the internal standard cocktail with the appropriate compounds, a commercially available C12-sulfatide (C12-ST) was used to quantify the sulfatides in the RAW264.7 cells. The highest recoveries of these compounds were obtained in the single-phase extract fraction; therefore, it was consistently used for analysis of these compounds (although the lower phase organic solvent extract could also be used, with this caveat).

The negatively charged sulfate product ion is highly abundant (supplementary Fig. V). Comparison of the signal responses for sulfatides on the API 3000 and 4000 QTrap (supplementary Fig. XI) revealed that the latter was approximately one order of magnitude more sensitive than the former (c.f. supplementary Fig. XI, panels A and B). Under optimized ionization conditions (Tables 3 and 4), the signal response was almost identical for C12-, C16:0- and C24:0-ST, and linear (0.5–1000 pmol) for both instruments. Similar comparisons with dihydro-ST and  $\alpha$ -hydroxy-fatty acid-containing ST were not possible due to lack of the necessary standards.

#### Analysis of sphingolipids in RAW 264.7 cells

RAW264.7 cells were used to test these methods and standards with cells in culture. First, the major molecular subspecies of the cells were determined (defined as variants in backbone composition that account for at least 1% of that category of sphingolipid), and the extraction and analysis efficiencies of the endogenous analytes and internal standards were examined, then several independent cultures of the cells were analyzed and the results compared.

*Identification of sphingolipid subspecies in RAW264.7 cells.* Before using MRM to quantify the sphingolipids in cells, the molecular subspecies were determined by precursor ion scans to ensure the protocol included all of the relevant MRM pairs. This was first accomplished by syringe infusion of the sample dissolved in 1 ml of CH<sub>3</sub>OH/HCOOH (99/1) (v/v) with 5 mM ammonium formate and (a) precursor ion scans of  $m/z$  184.4 to detect SM chain length variants (the profile for RAW 264.7 cells is shown in Fig. 7A); and (b) precursor scans of  $m/z$  264.4 and 266.4 over a wide range of collision energies (35–75 eV) to check for other classes of sphingolipids and the corresponding subspecies (Cer, HexCer, LacCer, etc.) (Fig. 7B). By these analyses, the major amide-linked fatty acids were C16:0, C18:0, C20:0, C22:0, C24:1, and C24:0, with very low amounts of C26:1 and C26:0 (and even lower amounts of C14:0 and C18:1, which were detectable but are not reported here because they were less than 1% of the total). The signals for C12 species were not detectable over background (Fig. 7); therefore, this chain length could be used for internal standards.

Precursor ion scans for other backbone sphingoid bases (e.g., phytosphingosine and other chain length homologs) were also performed as described previously (15, 34),<sup>8</sup> but

<sup>8</sup>“Phytosphingosines” (4-hydroxysphinganine) are detected as 16 u higher precursor ions that fragment to product ions of  $m/z$  282.4 and 264.4 (triple dehydration) and are distinguishable from sphingosines by LC migration; 3-ketosphinganine by fragmentation to  $m/z$  270.2 (for the d18:0 homolog) and LC mobility.

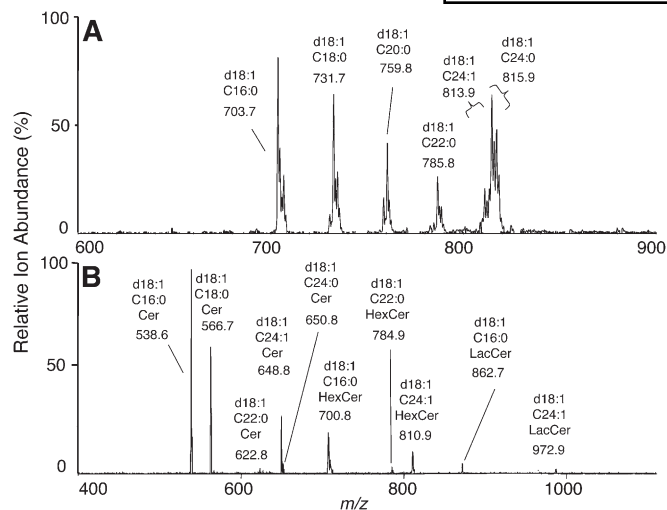


**Fig. 7.** Precursor ion scans of RAW264.7 cells using the 4000 QTrap. The lower phase extract from approximately  $10^6$  RAW264.7 cells was infused in methanol and precursors ions that fragment to  $m/z$  184.4 (panel A, sphingomyelins) and  $m/z$  264.4 (panel B, Cer, HexCer and LacCer) are shown.

none were found to be present in significant amounts (i.e., over 1%).

Other analytes can also be surveyed by such scans, such as sulfatides via precursor  $m/z$  96.9 scans. When applied to RAW264.7, no subspecies of sulfatide was significantly above the background. However, when the RAW264.7 cells were activated with Kdo<sub>2</sub>-Lipid A for 24 h (following the LIPID MAPS protocol described on [www.lipidmaps.org](http://www.lipidmaps.org)), the amounts were more substantial and included a Cer backbone with an  $\alpha$ -OH fatty acid, as described herein (**Fig. 10**).

**Analysis of the extraction efficiencies.** The use of an internal standard is based on the assumption that the behavior of the selected compound(s) will be similar not only for LC ESI-MS/MS (as has been shown to be the case for the compounds described herein) but also during the extraction procedures leading up to the analysis. Shown in **Figs. 8 and 9** are the recoveries of the internal standards and endogenous sphingolipids in sequential reextractions of RAW264.7 cells as described in “Materials and Methods.” To obtain the pmol shown, the integrated areas from the MRM analysis of each of the internal standards were compared with the areas for the internal standards analyzed directly (i.e., without extraction). It is evident that in essentially every case, over 90% of the internal standard spike (500 pmol) as well as each subspecies of analyte are recovered in the first and second extracts (which are pooled in the standard extraction protocol), with very little being lost in subsequent extracts. Furthermore, there are no noteworthy differences in the behavior of the internal standards and the cellular sphingolipids, although it is impossible to exclude the possibility that some of the endogenous sphingolipids are trapped in aggregates that are inaccessible to the extraction solvents.

**Estimation of the coefficient of variation for analysis of RAW264.7 cells.** The coefficients of variation (CV) for anal-

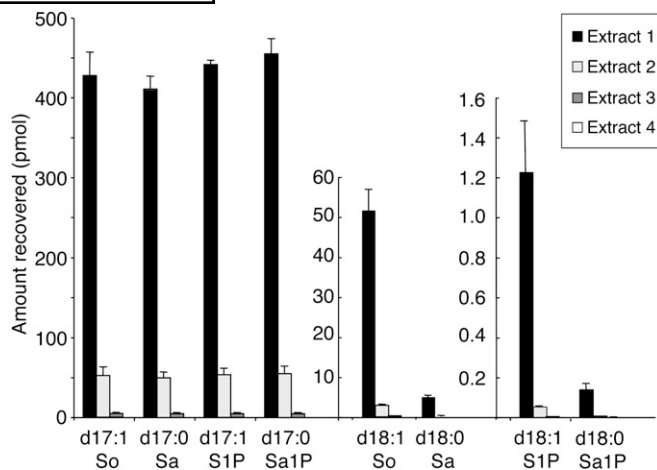


**Fig. 8.** Recovery of internal standards and cellular sphingoid bases and 1-phosphates at each cycle of extraction. Approximately  $1 \times 10^6$  RAW264.7 cells (approximately 3  $\mu$ g DNA) were spiked with the internal standard cocktail (500 pmol each), extracted four times, and analyzed using LC-MS/MS on an 4000 QTrap mass spectrometer as described under “Materials and Methods.” The amounts of the analytes in each extract were calculated using the MRM areas for the unknowns versus the areas for the internal standards injected directly (i.e., without extraction). The bars represent the mean  $\pm$  SD for  $n = 6$ .

ysis of Cer, GlcCer, and SM using these methods were determined using three separate cultures of cells (with six individual dishes per culturing) and were  $8 \pm 4\%$  for SM and somewhat higher ( $12 \pm 5\%$ ) for the less abundant Cer and HexCer, except when the subspecies was below 1 pmol/ $\mu$ g DNA, which increased the CV as much as 2-fold (supplementary Fig. XII). The CV for the sphingoid bases were 15–25% (also depending on abundance) (supplementary Fig. XIII), and for CerP, were as high as 50% (not shown), which might be due to the very low amounts of these metabolites or possibly dish-to-dish variation in the amounts, as this compound is thought to function mainly in cell signaling.

**Amounts of sphingolipids in RAW264.7 cells.** **Fig. 10** summarizes all of the subspecies of sphingolipids that have been analyzed in RAW264.7 cells using the methods described in this article. The results have many interesting features, such as: *a*) the relative amounts of the different sphingolipid subcategories, with SM being most abundant, followed by Cer and HexCer in about an order-of-magnitude lower amounts, then sphingosine and even smaller amounts of the other sphingoid bases and 1-phosphates, and Cer-1P; *b*) the high proportion of C16-dihydroCer (d18:0/C16:0) versus C16-Cer (d18:1/C16:0) compared with the other chain length (DH)Cer in any of the sphingolipid subcategories (Cer, SM, and HexCer); *c*) the noticeable differences in the (DH)Cer fatty acyl-chain lengths among the sphingolipid subcategories; *d*) the higher amounts of sphingosine versus sphinganine, and relative to the 1-phosphates; *e*) the presence of a substantial amount of an  $\alpha$ -hydroxy fatty acid (hC24:1) in the Cer backbone of sulfatides but none of the other lipid subcat-

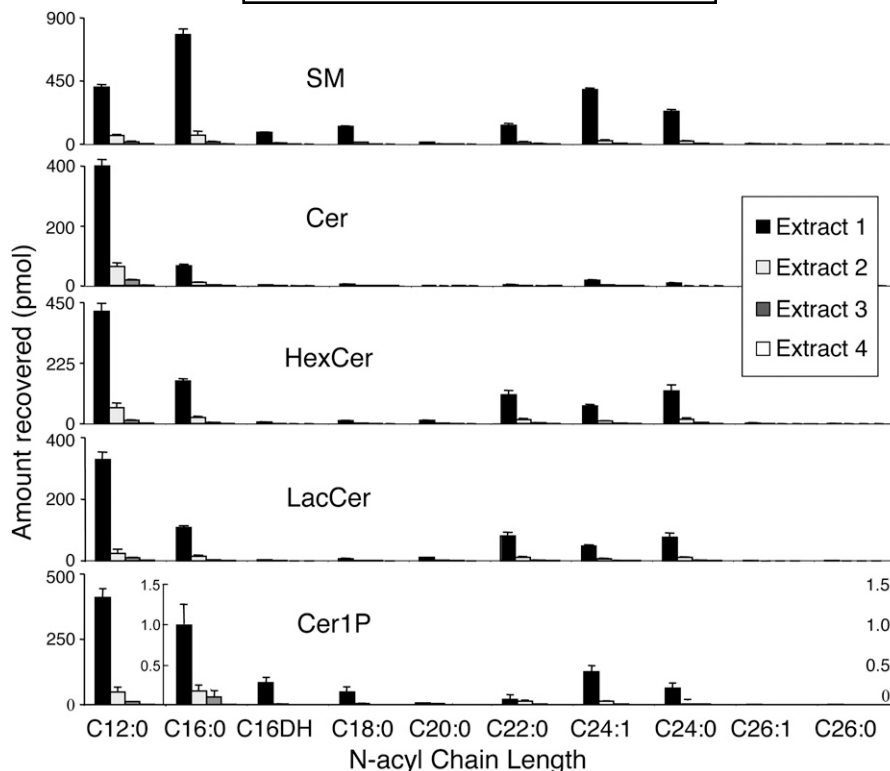


**Fig. 9.** Recovery of complex sphingolipids at each cycle of extraction. Approximately  $1 \times 10^6$  RAW264.7 cells (approximately  $3 \mu\text{g}$  DNA) were spiked with the internal standard cocktail (500 pmol of each species), extracted four times, and analyzed using LC-MS/MS on a 4000 QTrap mass spectrometer as described under “Materials and Methods.” The amounts of the analytes in each extract were calculated using the MRM areas for the unknowns versus the areas for the internal standards injected directly (i.e., without extraction). The bars represent the mean  $\pm$  SD for  $n = 6$ .

egories; and *f*) the absence of detectable sulfatides in RAW264.7 cells until activation by Kdo<sub>2</sub>-Lipid A. It also warrants comment that reanalysis of the monohexosylCer to determine the amounts of GlcCer versus GalCer (using the normal phase conditions shown in Figs. 1 and 2 and described under “Materials and Methods”) found that GlcCer accounted for approximately 90% ( $28.1 \pm 1.9$  pmol/ $\mu\text{g}$  DNA) versus 10% for GalCer ( $3.2 \pm 0.6$  pmol/ $\mu\text{g}$  DNA). The amounts of dihexosylCer were also low [(about half of HexCer (c.f. Fig. 9)]. A full description (and interpretation) of the sphingolipid composition of these is outside the scope of this article.

## DISCUSSION

This study has established methods for the quantitative analysis of all of the components of the sphingolipid metabolic pathway through backbone (Cer) and its initial metabolites (SM, GlcCer, GalCer, and Cer-P), including the sphingoid bases involved in sphingolipid turnover and cell signaling (sphingosine and SIP). A welcome finding was that a relatively small number of internal standards are needed to quantify these compounds using optimized LC ESI-MS/MS conditions, and as these are available commercially as a single cocktail, this should facilitate studies of this spectrum of metabolites. Of course, when using these internal standards for other applications, care should

be taken to ensure that none of the components are already present in the samples (for example, C17-sphingoid bases, which are found in some organisms—in which case one might obtain another standard, such as the C10- or C14-homolog, which is available from Matreya) (39) and that they are appropriate for any additional analytes beyond the ones validated in this study (for example, sphingolipids with “phyto”ceramide backbones). In addition, the amounts of the internal standard cocktail can be varied based on the analytes that are of greatest interest. In the case of this study, the internal standard cocktail was tailored to the most abundant analyte (SM); however, other choices can be made based on the experience of investigators with their particular application.<sup>9</sup>

Since multiple reaction monitoring only provides information about the specific precursor-product pairs that have been selected, it is important to begin by identifying the molecular species that are present in each new biological material and to recheck the composition when the cells

<sup>9</sup>We have examined cells that were spiked with 5, 50 or 500 pmol of the internal standards and the latter two resulted in the same analyte quantitations as are shown in Fig. 11; therefore, use of a lower amount of the internal standards (i.e., 50 pmol) might be preferable since this would place each internal standard within an order of magnitude of its respective analyte. One also has the option of formulating an internal standard cocktail with different amounts of the standards.

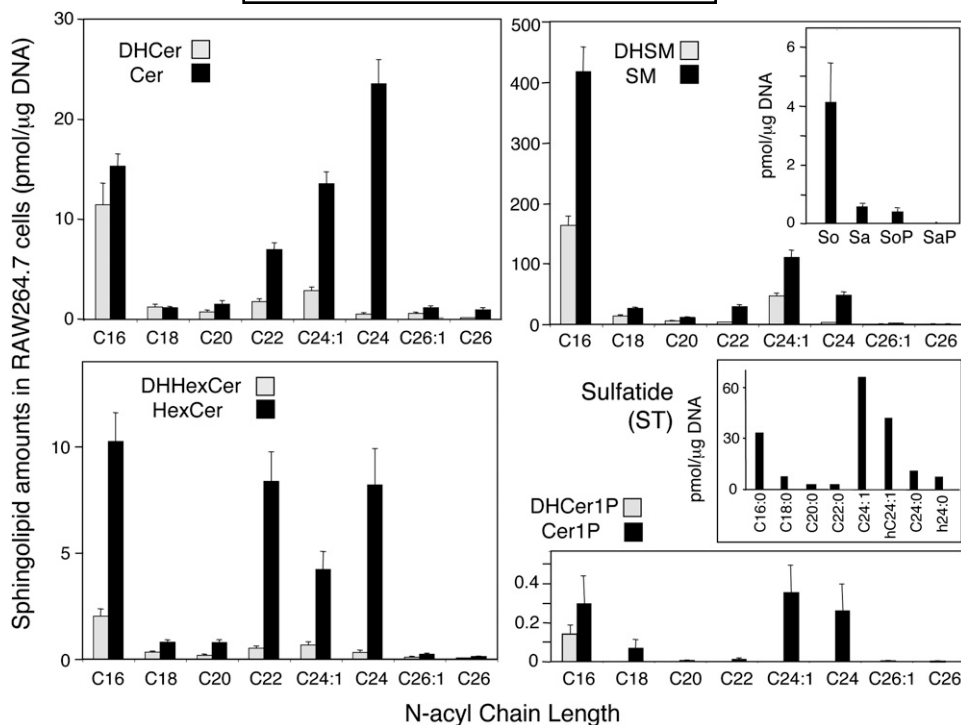


**Fig. 10.** Quantitative analysis of sphingolipids and dihydro sphingolipids in RAW264.7 cells. The amounts of these lipids were measured by LC-MS/MS using the internal standard cocktail as described under “Materials and Methods.” Shown are the means  $\pm$  SE ( $n = 18$ ) for three separate experiments with 6 dishes each. The upper insert shows the free sphingoid bases and 1-phosphates; the lower insert shows the amounts of sulfatides (ST) determined in an experiment where ST biosynthesis was induced by Kdo<sub>2</sub>-Lipid A, as described in the text. The N-acyl-chains of ST included hydroxy-24:1 (h24:1) and -24:0 (h24:0).

are treated in ways that might alter the composition, as illustrated in these studies by the appearance of quantifiable amounts of sulfatides only after the RAW264.7 cells have been treated with Kdo<sub>2</sub>-Lipid A. It is fairly easy to survey the types of sphingoid base backbones by starting with precursor ion scans for  $m/z$  264.4 and 266.4 as signatures for the sphingosine (d18:1) and sphinganine (d18:0), respectively (39).<sup>10</sup> The same principle is followed in scanning for sphingoid bases that differ in alkyl chain length (e.g.,  $m/z$  292.4 for eicosasphingosine, d20:1) and unsaturation (e.g.,  $m/z$  262.4 for sphingadienes that have been found in mammals and are more prevalent in plants) (40). “Phyto” (4-hydroxy-) sphingolipids often yield fragments with the same product  $m/z$  as sphingosines, but they can be distinguished by both their increased mass and retention time by LC (34). These precursor scans also provide information about the amide linked fatty acids, including special subcategories such as  $\alpha$ -hydroxy species (41). Once the sphingoid bases and N-acyl variants are known, the corresponding transitions can be incorporated into a new MRM protocol.

In optimizing the LC and mass spectrometer settings for analysis of large numbers of compounds using the selected

MRM protocol, the potential for two or more compounds having overlapping precursor-product ion pairs becomes considerable. In addition, the overlap can occur with not just the nominal mass of the compounds but also with isotopologues (for example, the  $M + 2$  <sup>13</sup>C isotopologue of d18:1 with d18:0) and ions that are produced by in-source degradation—and even the combination of both of these possibilities, as was found for C25-Cer in these studies. This argues strongly for use of a preMS separation method such as LC to reduce the likelihood of such artifacts as well as to confirm the identity of the analytes.

LC has the additional advantages that it *a*) reduces the complexity of the electrospray droplet, thereby decreasing the likelihood that it will be composed of compounds with greatly different gas phase basicity or acidity, which can suppress the ionization of the analyte(s) of interest (42); *b*) separates salts in the biological extract from the compounds of interest; hence, it minimizes formation of multiple salt adducts and other sources of ionization suppression (43); *c*) concentrates the analytes of interest in a small volume; and *d*) with appropriate choice of LC conditions, separates isomers that might not be distinguished by MS or MS/MS alone (44, 45).

In comparing the results with these mass spectrometers, several interesting differences were observed. For some of the compounds, the instruments produce different modes of fragmentation, such as the formation of  $m/z$  60.1 as a significant product from sphinganine in the 4000 QTrap. Signal response was also different for most of the com-

<sup>10</sup>This is less true for SM since of the phosphocholine headgroup produces a fragment that does not distinguish the components of the lipid backbone, however, as described under “Results” the backbone composition can be determined using the 4000 QTrap in an atypical ion selection/fragmentation mode.

pounds on the 4000 QTrap versus the API 3000, with the 4000 QTrap often being 3 to 4 orders of magnitude more sensitive than the API 3000. This increased sensitivity is most likely attributed to a combination of the orthogonal ion source and improved ion optics of the 4000 QTrap.

Although each new application of this methodology will require some degree of revalidation of these parameters, it is hoped that this provides a useful platform for lipidomics analysis of most, if not all, of the sphingolipids in the early steps of the metabolic pathway. The availability of an internal standard cocktail that is applicable to such a wide profile of compounds will not only facilitate such studies but will help ensure that the results from different laboratories can be compared. ■

The authors thank Dayanjan S. Wijesinghe, Nadia F. Lamour, and Charles E. Chalfant for bringing to attention that careful neutralization is important, as they have recently found that incorrect quantitation of CerP can result from SM hydrolysis if this is not done. The authors thank Avanti Polar Lipids for many of the compounds used to validate the internal standards.

## REFERENCES

- Lahiri, S., and A. H. Futerman. 2007. The metabolism and function of sphingolipids and glycosphingolipids. *Cell. Mol. Life Sci.* **64**: 2270–2284.
- Merrill, A. H., Jr., M. D. Wang, M. Park, and M. C. Sullards. 2007. (Glyco)sphingolipidology: an amazing challenge and opportunity for systems biology. *Trends Biochem. Sci.* **32**: 457–468.
- van Echten-Deckert, G. 2000. Sphingolipid extraction and analysis by thin-layer chromatography. *Methods Enzymol.* **312**: 64–79.
- Muthing, J. 2000. Analyses of glycosphingolipids by high-performance liquid chromatography. *Methods Enzymol.* **312**: 45–64.
- Mano, N., Y. Oda, K. Yamada, N. Asakawa, and K. Katayama. 1997. Simultaneous quantitative determination method for sphingolipid metabolites by liquid chromatography/ion spray ionization tandem mass spectrometry. *Anal. Biochem.* **244**: 291–300.
- Sullards, M. C. 2000. Analysis of sphingomyelin, glucosylceramide, ceramide, sphingosine, and sphingosine 1-phosphate by tandem mass spectrometry. *Methods Enzymol.* **312**: 32–45.
- Sullards, M. C., and A. H. Merrill, Jr. 2001. Analysis of sphingosine 1-phosphate, ceramides, and other bioactive sphingolipids by high-performance liquid chromatography-tandem mass spectrometry. *Sci. STKE.* **2001**: PL1.
- Lieser, B., G. Liebisch, W. Drobnik, and G. Schmitz. 2003. Quantification of sphingosine and sphinganine from crude lipid extracts by HPLC electro spray ionization tandem mass spectrometry. *J. Lipid Res.* **44**: 2209–2216.
- Ann, Q., and J. Adams. 1993. Structure-specific collision-induced fragmentations of ceramides cationized with alkali-metal ions. *Anal. Chem.* **65**: 7–13.
- Liebisch, G., W. Drobnik, M. Reil, B. Trumbach, R. Arnecke, B. Olgemoller, A. Roscher, and G. Schmitz. 1999. Quantitative measurement of different ceramide species from crude cellular extracts by electro spray ionization tandem mass spectrometry (ESI-MS/MS). *J. Lipid Res.* **40**: 1539–1546.
- Han, X. 2002. Characterization and direct quantitation of ceramide molecular species from lipid extracts of biological samples by electro spray ionization tandem mass spectrometry. *Anal. Biochem.* **302**: 199–212.
- Pettus, B. J., A. Bielawska, B. J. Kroesen, P. D. Moeller, Z. M. Szulc, Y. A. Hannun, and M. Busman. 2003. Observation of different ceramide species from crude cellular extracts by normal-phase high-performance liquid chromatography coupled to atmospheric pressure chemical ionization mass spectrometry. *Rapid Commun. Mass Spectrom.* **17**: 1203–1211.

- Karlsson, A. A., P. Michelsen, and G. Odham. 1998. Molecular species of sphingomyelin: determination by high-performance liquid chromatography/mass spectrometry with electrospray and high-performance liquid chromatography/tandem mass spectrometry with atmospheric pressure chemical ionization. *J. Mass Spectrom.* **33**: 1192–1198.
- Isaac, G., D. Bylund, J. E. Mansson, K. E. Markides, and J. Bergquist. 2003. Analysis of phosphatidylcholine and sphingomyelin molecular species from brain extracts using capillary liquid chromatography electro spray ionization mass spectrometry. *J. Neurosci. Methods.* **128**: 111–119.
- Merrill, A. H., Jr., M. C. Sullards, J. C. Allegood, S. Kelly, and E. Wang. 2005. Sphingolipidomics: high-throughput, structure-specific, and quantitative analysis of sphingolipids by liquid chromatography tandem mass spectrometry. *Methods.* **36**: 207–224.
- Shimizu, A., Y. Ashida, and F. Fujiwara. 1991. Measurement of the ratio of lecithin to sphingomyelin in amniotic fluid by fast atom bombardment mass spectrometry. *Clin. Chem.* **37**: 1370–1374.
- Brugger, B., G. Erben, R. Sandhoff, F. T. Wieland, and W. D. Lehmann. 1997. Quantitative analysis of biological membrane lipids at the low picomole level by nano-electrospray ionization tandem mass spectrometry. *Proc. Natl. Acad. Sci. USA.* **94**: 2339–2344.
- Pulfer, M., and R. C. Murphy. 2003. Electro spray mass spectrometry of phospholipids. *Mass Spectrom. Rev.* **22**: 332–364.
- Suzuki, M., M. Sekine, T. Yamakawa, and A. Suzuki. 1989. High-performance liquid chromatography-mass spectrometry of glycosphingolipids: I. Structural characterization of molecular species of GlcCer and IV3 beta Gal-Gb4Cer. *J. Biochem.* **105**: 829–833.
- Fujiwaki, T., S. Yamaguchi, M. Tasaka, N. Sakura, and T. Taketomi. 2002. Application of delayed extraction-matrix-assisted laser desorption ionization time-of-flight mass spectrometry for analysis of sphingolipids in pericardial fluid, peritoneal fluid and serum from Gaucher disease patients. *J. Chromatogr. B Biomed. Appl.* **776**: 115–123.
- Larson, G., and B. E. Samuelsson. 1980. Blood group type glycosphingolipids of human cord blood erythrocytes. *J. Biochem.* **88**: 647–657.
- Suzuki, Y., M. Suzuki, E. Ito, N. Goto-Inoue, K. Miseki, J. Iida, Y. Yamazaki, M. Yamada, and A. Suzuki. 2006. Convenient structural analysis of glycosphingolipids using MALDI-QIT-TOF mass spectrometry with increased laser power and cooling gas flow. *J. Biochem.* **139**: 771–777.
- Sweeley, C. C., and G. Dawson. 1969. Determination of glycosphingolipid structures by mass spectrometry. *Biochem. Biophys. Res. Commun.* **37**: 6–14.
- Karlsson, K. A., I. Pascher, and B. E. Samuelsson. 1974. Analysis of intact gangliosides by mass spectrometry. Comparison of different derivatives of a hematoside of a tumour and the major monosialoganglioside of brain. *Chem. Phys. Lipids.* **12**: 271–286.
- Arita, M., M. Iwamori, T. Higuchi, and Y. Nagai. 1983. Negative ion fast atom bombardment mass spectrometry of gangliosides and asialo gangliosides: a useful method for the structural elucidation of gangliosides and related neutral glycosphingolipids. *J. Biochem.* **94**: 249–256.
- Muthing, J., H. Egge, B. Kniep, and P. F. Muhlrardt. 1987. Structural characterization of gangliosides from murine T lymphocytes. *European Journal of Biochemistry / FEBS.* **163**: 407–416.
- Suzuki, M., T. Yamakawa, and A. Suzuki. 1991. A micro method involving micro high-performance liquid chromatography-mass spectrometry for the structural characterization of neutral glycosphingolipids and monosialogangliosides. *J. Biochem.* **109**: 503–506.
- Chen, S., G. Pieraccini, and G. Moneti. 1991. Quantitative analysis of the molecular species of monosialogangliosides by continuous-flow fast-atom bombardment mass spectrometry. *Rapid Commun. Mass Spectrom.* **5**: 618–621.
- Ivleva, V. B., L. M. Sapp, P. B. O'Connor, and C. E. Costello. 2005. Ganglioside analysis by thin-layer chromatography matrix-assisted laser desorption/ionization orthogonal time-of-flight mass spectrometry. *J. Am. Soc. Mass Spectrom.* **16**: 1552–1560.
- Leverly, S. B. 2005. Glycosphingolipid structural analysis and glycosphingolipidomics. *Methods Enzymol.* **405**: 300–369.
- Han, X., and H. Cheng. 2005. Characterization and direct quantitation of cerebroside molecular species from lipid extracts by shotgun lipidomics. *J. Lipid Res.* **46**: 163–175.
- Bielawski, J., Z. M. Szulc, Y. A. Hannun, and A. Bielawska. 2006. Simultaneous quantitative analysis of bioactive sphingolipids by high-performance liquid chromatography-tandem mass spectrometry. *Methods.* **39**: 82–91.

33. Sommer, U., H. Herscovitz, F. K. Welty, and C. E. Costello. 2006. LC-MS-based method for the qualitative and quantitative analysis of complex lipid mixtures. *J. Lipid Res.* **47**: 804–814.
34. Sullards, M. C., J. C. Allegood, S. Kelly, E. Wang, C. A. Haynes, H. Park, Y. Chen, and A. H. Merrill, Jr. 2007. Structure-specific, quantitative methods for analysis of sphingolipids by liquid chromatography-tandem mass spectrometry: “inside-out” sphingolipidomics. *Methods Enzymol.* **432**: 83–115.
35. Moore, J. D., W. V. Caufield, and W. A. Shaw. 2007. Quantitation and standardization of lipid internal standards for mass spectrometry. *Methods Enzymol.* **432**: 351–367.
36. Schwarzmann, G. 1978. A simple and novel method for tritium labeling of gangliosides and other sphingolipids. *Biochim. Biophys. Acta.* **529**: 106–114.
37. Raschke, W. C., S. Baird, P. Ralph, and I. Nakoinz. 1978. Functional macrophage cell lines transformed by Abelson leukemia virus. *Cell.* **15**: 261–267.
38. Boath, A., C. Graf, E. Lidome, T. Ullrich, P. Nussbaumer, and F. Bornancin. 2008. Regulation and traffic of ceramide 1-phosphate produced by ceramide kinase: comparative analysis to glucosylceramide and sphingomyelin. *J. Biol. Chem.* **283**: 8517–8526.
39. Pruetz, S. T., A. Bushnev, K. Hagedorn, M. Adiga, C. A. Haynes, M. C. Sullards, D. C. Liotta, and A. H. Merrill, Jr. 2008. Sphingolipids. Biodiversity of sphingoid bases (“sphingosines”) and related amino alcohols. *J. Lipid Res.* **49**: 1621–1639.
40. Sullards, M. C., D. V. Lynch, A. H. Merrill, Jr., and J. Adams. 2000. Structure determination of soybean and wheat glucosylceramides by tandem mass spectrometry. *J. Mass Spectrom.* **35**: 347–353.
41. Masukawa, Y., H. Tsujimura, and H. Narita. 2006. Liquid chromatography-mass spectrometry for comprehensive profiling of ceramide molecules in human hair. *J. Lipid Res.* **47**: 1559–1571.
42. Pettus, B. J., B. J. Kroesen, Z. M. Szulc, A. Bielawska, J. Bielawski, Y. A. Hannun, and M. Busman. 2004. Quantitative measurement of different ceramide species from crude cellular extracts by normal-phase high-performance liquid chromatography coupled to atmospheric pressure ionization mass spectrometry. *Rapid Commun. Mass Spectrom.* **18**: 577–583.
43. Tsui, Z. C., Q. R. Chen, M. J. Thomas, M. Samuel, and Z. Cui. 2005. A method for profiling gangliosides in animal tissues using electrospray ionization-tandem mass spectrometry. *Anal. Biochem.* **341**: 251–258.
44. Ramstedt, B., and J. P. Slotte. 2000. Separation and purification of sphingomyelin diastereomers by high-performance liquid chromatography. *Anal. Biochem.* **282**: 245–249.
45. Muthing, J., and F. Unland. 1994. Improved separation of isomeric gangliosides by anion-exchange high-performance liquid chromatography. *J. Chromatogr. B Biomed. Appl.* **658**: 39–45.